Numerical modeling of seawater intrusion into endorheic hydrological systems

U. Kafri · E. Shalev · V. Lyakhovsky · S. Wollman · Y. Yechieli

Abstract Several groundwater endorheic base levels are known in different parts of the world. Some of them allow seawater encroachment into them. Two examples of such groundwater systems, at Lake Asal in the Afar Depression of East Africa and Lago Enriquillo in the Dominican Republic, have been modeled using FEFLOW. The simulated flow pattern reproduces the seawater encroachment all the way from the sea to the endorheic base level. When the water in that base level undergoes concentration to brine through evaporation, the dense brine starts to flow below the encroaching seawater body in the opposite direction toward the sea. These processes reach steady-state conditions in a relatively short time of several hundred years.

Keywords Groundwater flow · Numerical modeling · Endorheic base level · Seawater intrusion

Introduction

Seawater intrusion to coastal aquifers is a well known and described phenomenon from all over the world, extending to a limited inland distance from the sea. This process has been extensively studied over a century starting with pioneering papers by Ghyben (1888) and Herzberg (1901). Mathematical models for seawater intrusion into coastal aquifers have been discussed in several reviews (Reilly and Goodman 1985; Bobba 1993; Bear et al. 1999) and in many other papers (e.g., Essaid 1990; Harrar et al. 2001; Bobba 2002; Kooi et al. 2000; Ataie-Ashtiani et al. 1999; Chen and Hsu 2004). A groundwater base level was defined as a drainage level for the aquifer that represents the lowest groundwater level that will occur from groundwater flow only (Olin 1995). However, the specific situations whereby seawater intrudes the hydrological system across the groundwater divide into continental endorheic groundwater base levels or lakes located relatively far from the sea has seldom been described and modeled (Kafri and Arad 1979; Kafri (1984); Kafri et al. 2007; Kafri and Yechieli 2010).

Such base levels, which are below sea level, are known from all over the world (Kafri and Yechieli 2010). Being terminal base levels, they capture water from the surrounding area and may also be encroached by seawater. This possibility, originally proposed by Kafri and Arad (1979) for the Dead Sea Rift, was further analyzed for other places in the world (Kafri 1984; Kafri and Yechieli 2010). Seawater encroachment to areas with endorheic base levels below sea level was suggested to be feasible if the endorheic lake is located not too far from the sea, the elevation difference between the sea surface and base levels is significant, and the aquifer that connects the sea and the lake is thick enough. Kafri and Arad (1979) demonstrated that this mechanism is feasible for the northern Dead Sea Rift base level, which is 210–250 m below sea level (hereafter bsl) and located some 50 km from the Mediterranean Sea. A deep geo-electromagnetic study showed the configuration of the interface between the encroaching seawater and the overlying freshwater between the Mediterranean Sea and the Dead Sea Rift which was also supported by hydrological modeling (Kafri et al. 2007).

Based on the preceding, a working hypothesis is formulated for the hydrological configuration of those endorheic base levels, close and connected to the sea, which are below sea level (Fig. 1). A hydrological system is proposed consisting of an upper freshwater body that drains to both base levels, controlled by the fresh groundwater heads. Underneath it, seawater encroaches all the way from the sea to the lower inland base level whereby the geometry of the fresh/seawater interface formed is controlled by the elevation difference between both base levels, by the freshwater heads and by the densities of the two water bodies involved. Below it an interface is recognized between the encroaching seawater body and a brine body underneath, formed through evaporation in the endorheic base level and which is density-driven backwards toward the sea.

Received: 24 May 2012 / Accepted: 26 February 2013
Published online: 10 April 2013

U. Kafri · E. Shalev · V. Lyakhovsky (✉) · S. Wollman · Y. Yechieli
Geological Survey of Israel, 30 Malchei Israel St, Jerusalem, 95501, Israel
e-mail: vladi@gsi.gov.il
Tel.: +972-2-5314265
Fax: +972-2-5380688

 DOI 10.1007/s10040-013-0972-5

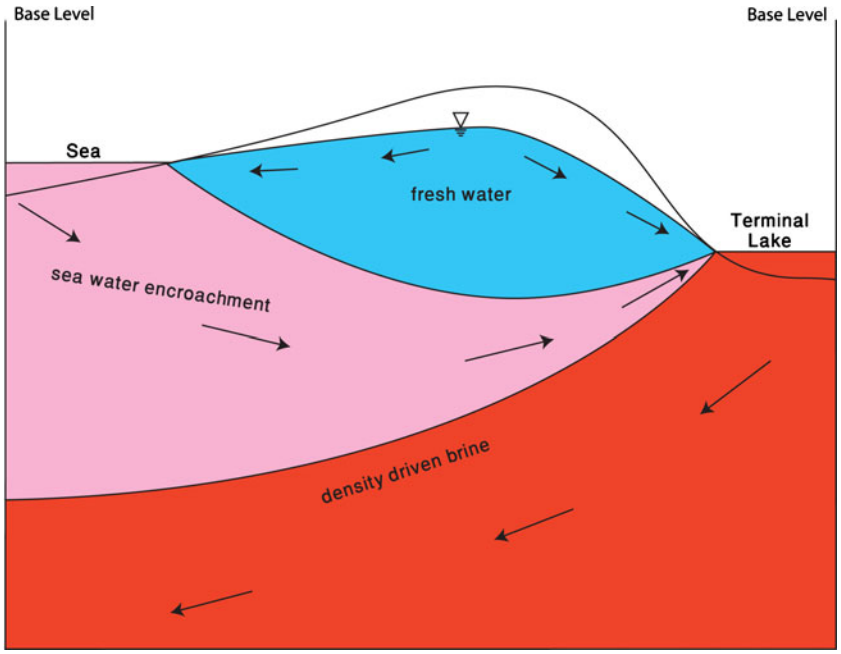

Fig. 1 A schematic conceptual model of a multiple hydrological configuration between the sea and a hyper-saline endorheic base level

The objective of the present study is to prove the validity of the proposed hypothesis by modeling two cases of such endorheic base levels, namely Lake Asal in the Afar Depression of East Africa and Lago Enriquillo in the Dominican Republic, previously described by Kafri and Yechieli (2010). It should be noted that the level of knowledge and the availability of data are different for the different endorheic basins. Uncertainty and non-uniqueness of the geological structure and the hydrological parameters often do not allow calibration of numerical modeling. The two examples, described herein, represent base level development from a different initial configuration, namely a freshwater lake and a sea arm in the cases of Lake Asal and Lago Enriquillo, respectively, both ending up as hypersaline endorheic base levels.

Numerical solution

In this section, numerical modeling is presented of two groundwater systems using FEFLOW, a finite element simulator (Diersch and Kolditz 2002). FEFLOW solves the coupled variable density and viscosity groundwater flow and solute and heat transport. The specific parameters for the two cases, namely Lake Asal and Lago Enriquillo, are given in Tables 1 and 2, respectively. The automatic adaptive time step procedure was applied. In all cases, flow boundary conditions were set to impermeable boundaries at the left, right and bottom boundaries. The top boundary condition was set as recharge at the land and prescribed hydraulic equivalent freshwater head at the lakes and sea, except for the area of submarine groundwater discharge near the shoreline, where zero salinity gradient was prescribed. The appropriate salinities were prescribed at the lakes and sea. The salinity at the recharge area was set to zero and the left, right and bottom boundaries were also impermeable for salt. In the first case of Lake Asal, temperatures were prescribed at the top and bottom boundaries. Left and right boundaries were impermeable for heat.

The Afar depression and Lake Asal

Site description and hydrogeology

The Afar, or Danakil Depression (Fig. 2), is a vast closed endorheic base level which is considerably below sea level and is located in the Horn of Africa, belonging to Ethiopia, Eritrea and Djibouti. The depression contains a series of lakes and salt pans at various depths below sea level. They are Lake Badda (−50 m), Lake Assale (−118 m), Lake Bakili (−120 m), Lake Afrera (−111 m), Lake Acori (−94 m) and the lowest Lake Asal (−155 m). The depression is located within the Afar triangle which is a triple junction between the Red Sea, the Gulf of Aden (Fig. 2) and the East African (or Main Ethiopian) Rift systems. The region is a plate boundary, part of the Afro-Arabian system, which is subjected to sea-floor spreading, rifting and recent tectonics, fissure openings, volcanism and hydrothermal activity (Allard et al. 1979; Tarantola et al. 1980; Audin et al. 2001; Manighetti et al. 2001; Wright et al. 2006; Pizzi et al. 2006; Ayele et al. 2006; Buck 2006; Garfunkel and Beyth 2006; Doubre and Peltzer 2007). The landward extension of the eastern segment of the transform of the triple junction, namely the Gulf of Aden, forms the Asal Rift, which extends inland from the Goubhet el Kharab seawater embayment (Mlynarski and Zlotnicki 2001). In general, this area is an active rift that consists mainly of a sequence of young volcanic rocks, to a depth exceeding 1,500 m. The geothermal field (thermal

 DOI 10.1007/s10040-013-0972-5

Table 1 Lake Asal model parameters

Model parameter	Value
Horizontal hydraulic conductivity	100 m/d
Vertical hydraulic conductivity	10 m/d
Recharge rate	20 mm/year
Compressibility of aquifer	1×10^{-5} 1/m
Porosity	0.2
Sea head relative to sea level	0 m
Lake head relative to sea level	+100 to −155 m
Seawater density	1.025 g/cm^3
Maximum brine density in lake	1.25 g/cm^3
Seawater concentration	35 g/l
Maximum brine concentration in lake	350 g/l
Temperature of lower aquifer boundary	350 °C
Temperature of upper aquifer boundary	25 °C
Heat capacity of fluid	4.2×10^6 J/m^3/K
Heat capacity of rock	2.52×10^6 J/m^3/K
Thermal conductivity of fluid	0.65 J/m/s/K
Thermal conductivity of rock	2.0 J/m/s/K
Thermal expansion coefficient	2×10^{-4} 1/K
Finite element size (triangular elements)	100 m
Total number of elements in finite element mesh	13,840

gradient and heat flow), based on data from boreholes in the study area, were described by Jalludin and Razack (1994), D'Amore et al. (1998) and Elmi (2005).

The most fascinating and the lowest base level (presently at 155 m bsl and at coordinates 11°N, 42° E,) is Lake Asal. This hypersaline lake serves as a terminal base level and has attracted the interest of several authors (e.g., Gasse and Fontes 1989). Its maximum and average depths are 40 and 7.4 m, respectively. The total salinity of its waters is around 350 g/l. Mean annual rainfall in the area is 175–200 mm/year and evaporation exceeds 3.5 m/year (Gasse and Fontes 1989). The lake is fed by groundwater (Gasse et al. 1980) and is located some 11–12 km from the Gulf of Aden and the Ghubbet el Kharab marine base level. The Lake Asal and Goubhet el Kharab base levels are separated by a rather shallow topographic divide in between, which is part of the tectonically active Afar Rift. As a result, the entire region, and specifically the divide, is subjected to fissure openings and the enlargement of fractures, and thus increased permeability (Allard et al. 1979; Kafri 1984; Gasse and Fontes 1989; Mlynarski and Zlotnicki 2001; Doubre and Peltzer 2007).

Table 2 Lago Enriquillo model parameters

Model parameter	Value
Horizontal hydraulic conductivity	400 m/d
Vertical hydraulic conductivity	400 m/d
Recharge rate	120 mm/year
Compressibility of aquifer	1×10^{-5} 1/m
Porosity	0.2
Seawater density	1.025 g/cm^3
Sea head relative to sea level	0 m
Lake head relative to sea level	−10 to −46 m
Maximum brine density in lake	1.075 g/cm^3
Seawater concentration	35 g/l
Maximum brine concentration in lake	105 g/l
Finite element size (triangular elements)	100 m
Total number of elements in finite element mesh	28,096

The paleohydrology of Lake Asal is described in detail by Gasse and Fontes (1989). According to their study (Fig. 3), the paleo Lake Asal was almost dry in the late Pleistocene, due to the arid conditions that prevailed at that time. They suggested a highstand lake level at 160 m above present day sea level (asl) that existed in the early Holocene, between 8.6 and 6 ka, draining to the sea. However, the present-day topographic divide between the sea and the lake is at 110 asl. If that was the topographic setup some 6,000 years ago, it would not have allowed the existence of a freshwater lake at 160 masl at that time and, thus, it is assumed that the setup was different, namely that the divide was higher. In order to overcome this apparent contradiction, in the model set-up (next section) the initial freshwater lake level at that time was set at 110 masl, matching the present-day topography. Subsequent to this time period, the lake level dropped rapidly, over some 300 years, to 155 mbsl (Fig. 3), enabling subsurface seawater infiltration from the sea to the lake across the fractured divide. Since then, the lake water salinity and that of the aquifer system between the lake and the sea have been controlled mainly by a mixture of thermal waters and encroaching seawater across the divide. The seawater contribution is also evidenced by the thermal Manda Springs waters of marine origin that issue on the shores of Lake Asal (Gasse et al. 1980; Kafri 1984; Fouillac et al. 1989; Gasse and Fontes 1989; Sanjuan et al. 1990; D'Amore et al. 1998; Faure et al. 2002; Elmi 2005; Kafri and Yechieli 2010). Mlynarski and Zlotnicki (2001) used geophysical data to describe the subsurface fluid circulation pattern between the sea and the Asal Rift, exhibiting large and rapid subsurface seawater fluid transfer from the sea to the lake along permeable fault zones or beds, warming up during their advance by the underlying geothermal flux. Concentrated brines of some 116 g/l TDS were detected in the Asal hydrothermal wells at a depth interval between 1,075 and 1,320 m (D'Amore et al. 1998; Houssein and Axelsson 2010).

Model setup

Based on the present-day geographic configuration and on hydrological and paleo-hydrological data coupled with the geothermal configuration, transient simulations were employed to exhibit the changes of the salinity fields of the hydrological system, taking into account the changing lake levels since ca. 6 ka (Fig. 3). The initial freshwater lake level at that time was set at 110 asl. The sea level was set at the beginning of the transient simulation as the present one since that was roughly the global sea level during the last millennia. The model parameters of Lake Asal are given in Table 1. The model size is 30,000 m from the sea in the east to the lake in the west. The base of the model was set at a 2,000 m depth bsl, which is the deepest source of hydrological available information. The recharge to the upper surface boundary was taken as 20 mm/year, assuming a recharge coefficient of ca.10 %, typical of arid regions. The sea side was set as normal seawater with salinity and density of 35 g/l and 1.025 g/cm^3, respectively. The lake side was set at an initial elevation of 110 m asl and an initial salinity and density of 0 g/l and 1 g/cm^3 respectively, representing freshwater. The lake level declined over 300 years by 265 m. The salinity of

 DOI 10.1007/s10040-013-0972-5

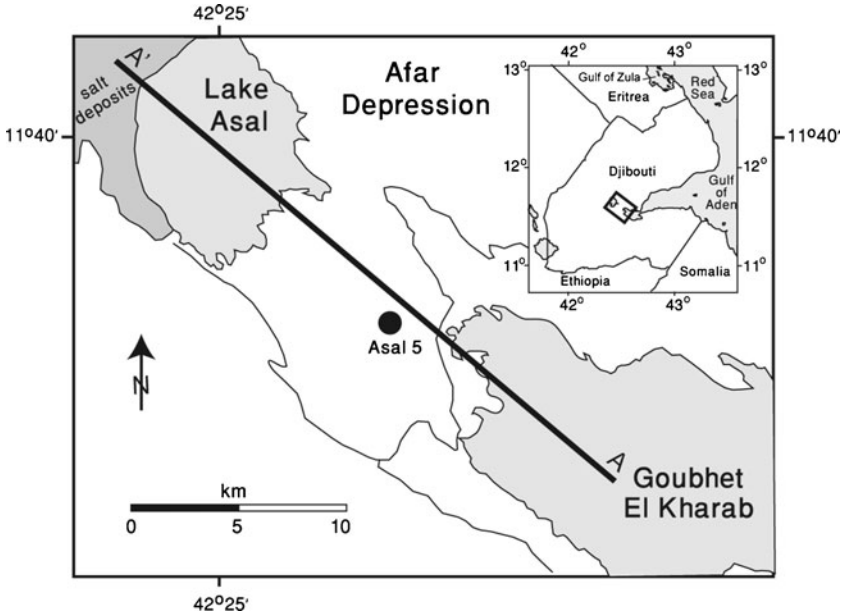

Fig. 2 Location map of the Afar Depression and *Lake Asal* as well as the location of the *Asal 5* well. The location of the simulated cross section between the sea and the lake (A′–A) is also shown

the lake was prescribed as freshwater (in terms of salinity) until the lake level reached the elevation of almost below sea level. From this point, the salinity was set to increase linearly to the final salinity during the aforementioned time span. The final present-day lake level was set at 155 m bsl and TDS salinity of 350 g/l. The horizontal and vertical hydraulic conductivity (K) values of 100 and 10 m/d, respectively, were based on data obtained from the hydrothermal field underneath the study area (Jalludin and Razack 1994; Elmi 2005). Temperature was set to 350 °C at the bottom boundary and to 25 °C at the upper boundary, based on data from Houssein and Axelsson (2010).

Results and discussion

Results of the transient simulation of the Lake Asal system demonstrate steady-state condition at the end of the initial stage (Fig. 4a). The configuration is of a freshwater lake in the west (right side of Fig. 4) at an elevation of 110 m asl and a seawater body in the east. The freshwater body occupied the lake and the aquifers underneath and extended to the east, resulting in a steady-state interface between the freshwater body and the seawater. The significant drop of the lake level (Fig. 4b) was accompanied by seawater encroachment all the way across and already below the hydrological divide to the

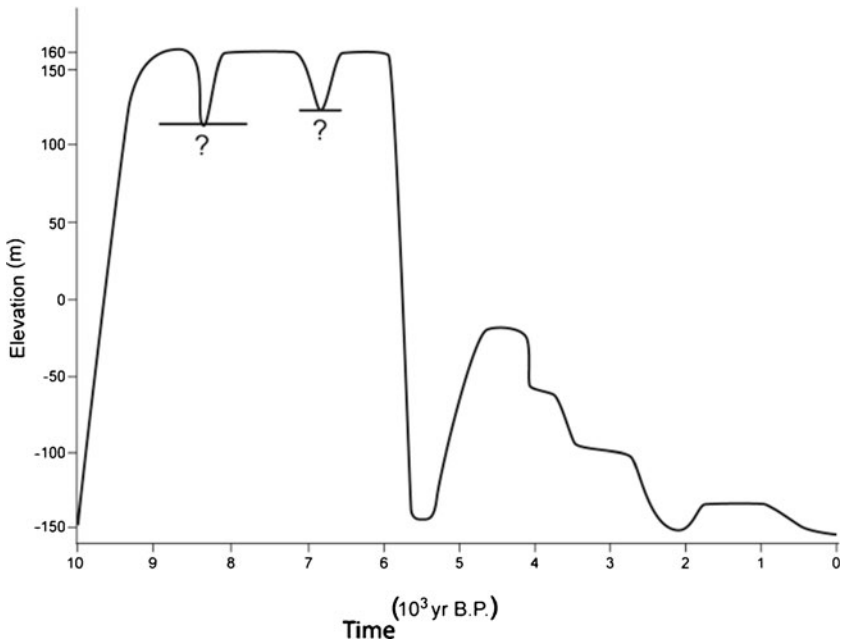

Fig. 3 Lake Asal levels over the last 10,000 years (modified after Gasse and Fontes 1989). The *question marks* represent uncertain levels marked in the original version

 DOI 10.1007/s10040-013-0972-5

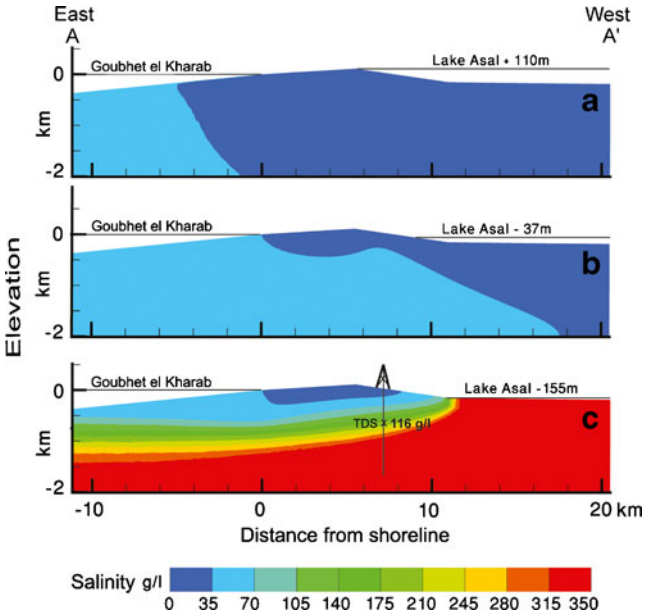

Fig. 4 Transient simulations of the salinity field changes between the sea and Lake Asal in relation to lake level changes. **a** Maximum lake level; **b** Lake level below sea level, where seawater starts to be discharged to the lake; and **c** Current situation where *X* denotes a total dissolved solids (*TDS*) value of 116 g/l, as detected in the hydrothermal wells

system below the lake when the lake level dropped to the elevation of 37 m below sea level. The subsequent drop from this lake level to the final, present-day steady state at 155 m asl (Fig. 4c) was accompanied by continuous seawater encroachment which already occupied the lake and the system underneath. Following the drop of the lake level, and the formation of a terminal lake, the water salinity of the system increased rapidly due to the high evaporation rate. The final steady-state configuration is that of an upper fresh groundwater body between the sea and the lake, underlain by an interface with the intruding seawater all the way to the lake. The concentrated (350 g/l) brine, formed in the lake, is being density-driven backwards toward the sea underneath the intruding seawater body. The system attains a steady-state condition after around 100 years, which is a short time as compared to the rate of the lake level changes. Thus, it is suggested that the present-day situation is at steady state. Since the hydraulic conductivity values are high, the fresh groundwater and density-driven brine flow velocities are quite high reaching values of several meters per year. Due to the short distance between both base levels, it may take only a few decades for seawater to arrive to the lower base level. In addition, assuming a typical specific storage value of 10^{-5} 1/m, the system establishes a steady-state flow pattern relatively fast (ca. 100 years) as compared to the rate of lake level decline. Therefore, the drop of the endorheic base level, as described in the preceding, is accompanied by an almost immediate consecutive steady-state salinity pattern at each time step.

The simulated salinity field is in agreement with the value of 116 g/l described from the hydrothermal field by D'Amore et al. (1998), Elmi (2005) and Houssein and Axelsson (2010), at a depth interval between ca. 1,000 and 1,300 m (Fig. 4c). Due to the known high regional heat flux, it was expected that the temperature significantly affects the water-flow pattern. Therefore, the next simulations were run for the coupled case whereby temperature and salinity are both taken into account. The resulting salinity and temperature fields are exhibited in Fig. 5. It should be noted that the temperature curve of the hydrothermal field (Fig. 6) exhibits a "reversal" at depth. This feature roughly mimics the phenomenon observed at the Asal 5 well (Houssein and Axelsson 2010). The upward component of the groundwater flows around the fresh/seawater interface and transports heat by convection from the hot, deeper parts of the reservoir to the colder surface and vise versa. Several other buoyancy-driven convection cells exist in the region due to the high geothermal heat flux, but only the cell created by the fresh/seawater interface creates such a reversal (Figs. 5 and 6).

The backward density-driven brine flow extends eastward all the way to underneath the Gulf of Aden area. It should be noted that hot brines were described from the "Deeps" of the Red Sea (e.g., Atlantic II Deep; Brewer and Spencer 1969), related to the sea floor spreading of the Red Sea and the Gulf of Aden. These brines were interpreted as a mixture of deep-seated concentrated brines with deep Red Sea water (e.g., Brewer and Spencer 1969). The brines were interpreted to migrate northward along the Red Sea all the way from the Gulf of Aden and the Bab el Mandeb Straits (Craig 1969; Schoell and Faber 1978) from offshore and close to the discussed area herein. It can be thus speculated that some of these brines could have originated from the Afar Triangle, below sea level, as exhibited in the Lake Asal model, and subsequently density-driven back to the Gulf of Aden, or northward by the same mechanism through the Gulf of Zula to the Red Sea and have emerged along the active fault system to the Red Sea bottom.

Lago Enriquillo

Site description and hydrogeology

Lago Enriquillo, in the Dominican Republic, at coordinates 18°N, 71°W, is a hypersaline lake, at an elevation of some 46 m below sea level, situated about 50 km west of the Caribbean Sea (Fig. 7). The lake is situated within an 85-km long and 12-km wide morpho-tectonic depression or rift valley named the Cul de Sac Depression, which extends from the Dominican Neiba embayment in the Caribbean Sea to Haiti in the west (Mann et al. 1984; Chiesa and Mazzoleni 2001). The area, which is situated within the boundary zone between the Caribbean plate and the North American plate, is transected by abundant active strike slip and reverse faults, which are responsible for the current seismic activity in the area (Mann et al. 1984; Tuttle et al. 2003; DeMets and Wiggins-Grandison 2007). The maximum and average depths of the lake are 20 and 6 m, respectively. The lake is laterally fed by groundwater from its adjoining aquifers whose natural recharge is ca. 120 mm/year (Morillo and Huertas 2006). According to data derived from internal

 DOI 10.1007/s10040-013-0972-5

reports, a sloping water table is recognized from east to west to levels below sea level toward the lake.

At the peak of the last glacial period, some 18,000 years ago, the Enriquillo depression, according to its present topography and the lake's bathymetry, was assumingly above sea level and draining to the considerably low global and Caribbean Sea base level at 120 m bsl, through the present day Neiba embayment (Mann et al. 1984). The subsequent rising sea level caused flooding in the Enriquillo depression, in the early Holocene time, at ca. 9.8 ka, creating an inland sea arm, which existed until ca. 4,900 ka. At around 4,900 ka, the marine sea arm was disconnected from the sea, as a result of the combination of damming of the eastern mouth of the valley by deltaic deposits, and possibly due to vertical movements. Following the restriction of the embayment, it became a closed hypersaline lagoon and its level dropped to the present one, below sea level, due to the high evaporation of this arid area and the continuous subsidence of the depression since then (Mann et al. 1984; Doss et al. 2005; Medley 2006; Winsor et al. 2006). The present total salinity, as well as the different ion concentrations and stable isotope composition of the lake water, were discussed in detail by Buck et al. (2005). The hypersaline nature of the water is related to evaporation as is also exhibited by the stable isotope composition. The total salinity of the lake water fluctuates annually and seasonally in response to recharge and evaporation. Historic salinities ranged from about 35 g/l (normal marine salinity) to over 100 g/l. At present, the total seasonal salinity range is between ca. 80 and 105 g/l with a concentration factor of 2.25 compared to Caribbean

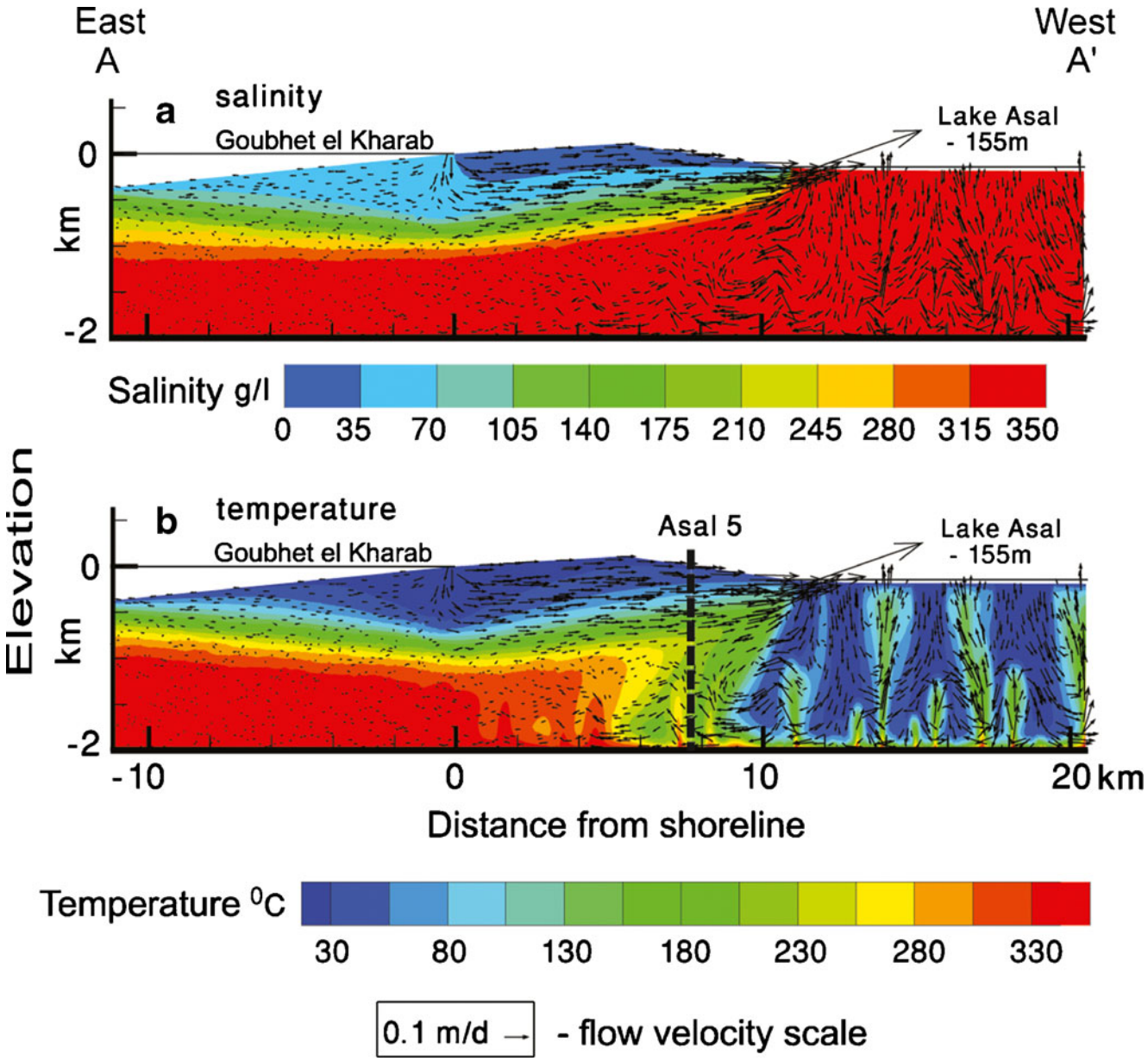

Fig. 5 Steady state simulation of **a** salinity and **b** temperature distribution between the sea and Lake Asal

 DOI 10.1007/s10040-013-0972-5

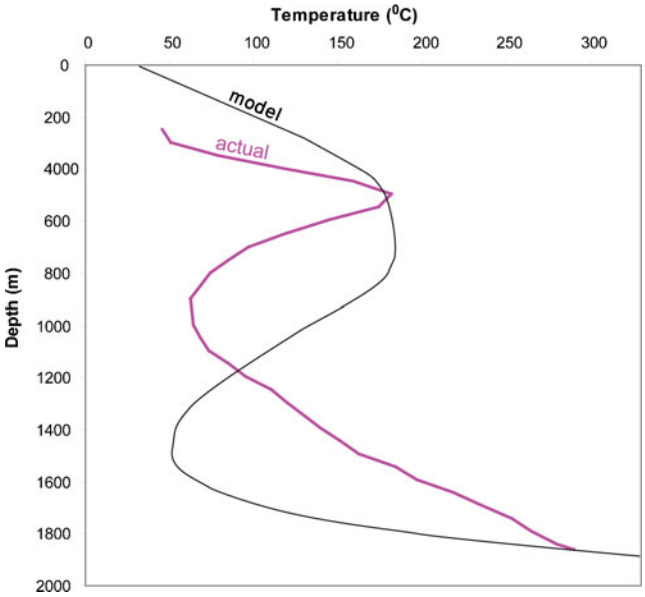

Fig. 6 Actual and modeled temperature curves of the Asal 5 well

seawater. It is interesting to note that the initial marine geochemical signature of the water is not obscured by the evaporation process, as shown by the calculated Na/Cl equivalent ratio, around 0.87, resembling that of the Caribbean seawater. It is suggested herein that the saline end member could be partly related to current subsurface seawater encroachment to this base level, which underwent evaporation, reaching a higher salinity than that of seawater (Kafri and Yechieli 2010).

Model setup

Based on the above data, a transient simulation was conducted (Fig. 8) in order to exhibit the changes that took place in the hydrological configuration since the detachment of the area from the sea and the start of decline of the newly formed endorheic lake level at 4,900 ka. The model parameters of Lago Enriquillo are given in Table 2. The model size is 100,000 m from the sea in the east to the lake in the west. The base of the model was set at 1,000 m depth. The recharge to the upper surface boundary was taken as 120 mm/year based on Morillo and Huertas (2006). The sea-side boundary was set at present sea level for both the steady-state condition and the initial of the transient simulation starting at 4,900 ka. Sea level was set to remain constant during the transient simulation. The lake-side level was set at 0 m (sea level) for the steady-state simulation. For the transient simulation, the lake level was declined linearly from 0 to 46 m bsl in 4,900 years. Simultaneously, the salinity was set to increase linearly from 35 to 105 g/l. The average of both the horizontal and vertical hydraulic conductivity was 400 m/d (E. Shachnai, Tahal Water Planning for Israel, personal communication, 2012).

Results and discussion

The results of the transient simulation of the Lago Enriquillo system exhibit the initial steady-state stage (Fig. 8a) where both base levels were occupied by normal seawater, overlain by a freshwater lens in between. A normal fresh/seawater interface is recognized. Following the decline of the lake level to become an endorheic base level (Fig. 8b), seawater encroached in from the sea and the lake's water salinity increased due to evaporation to form brine. An additional interface is recognized between the encroaching seawater and the underlying brine that is being density-driven toward the sea. The final (present day) state (Fig. 8c) exhibits an endorheic base level that

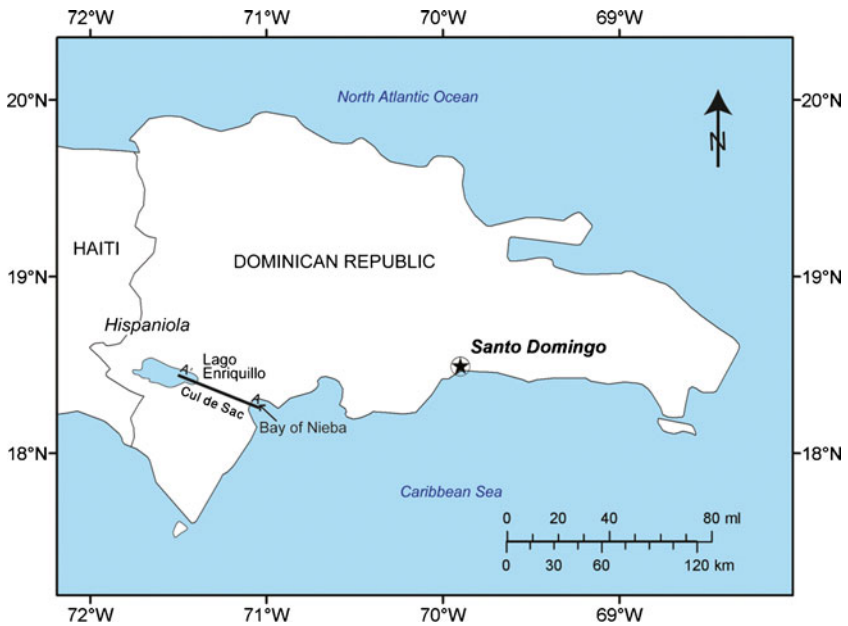

Fig. 7 Location map of Lago Enriquillo in the Dominican Republic. The location of the simulated cross-section (A′–A) between the sea and the lake is also shown

 DOI 10.1007/s10040-013-0972-5

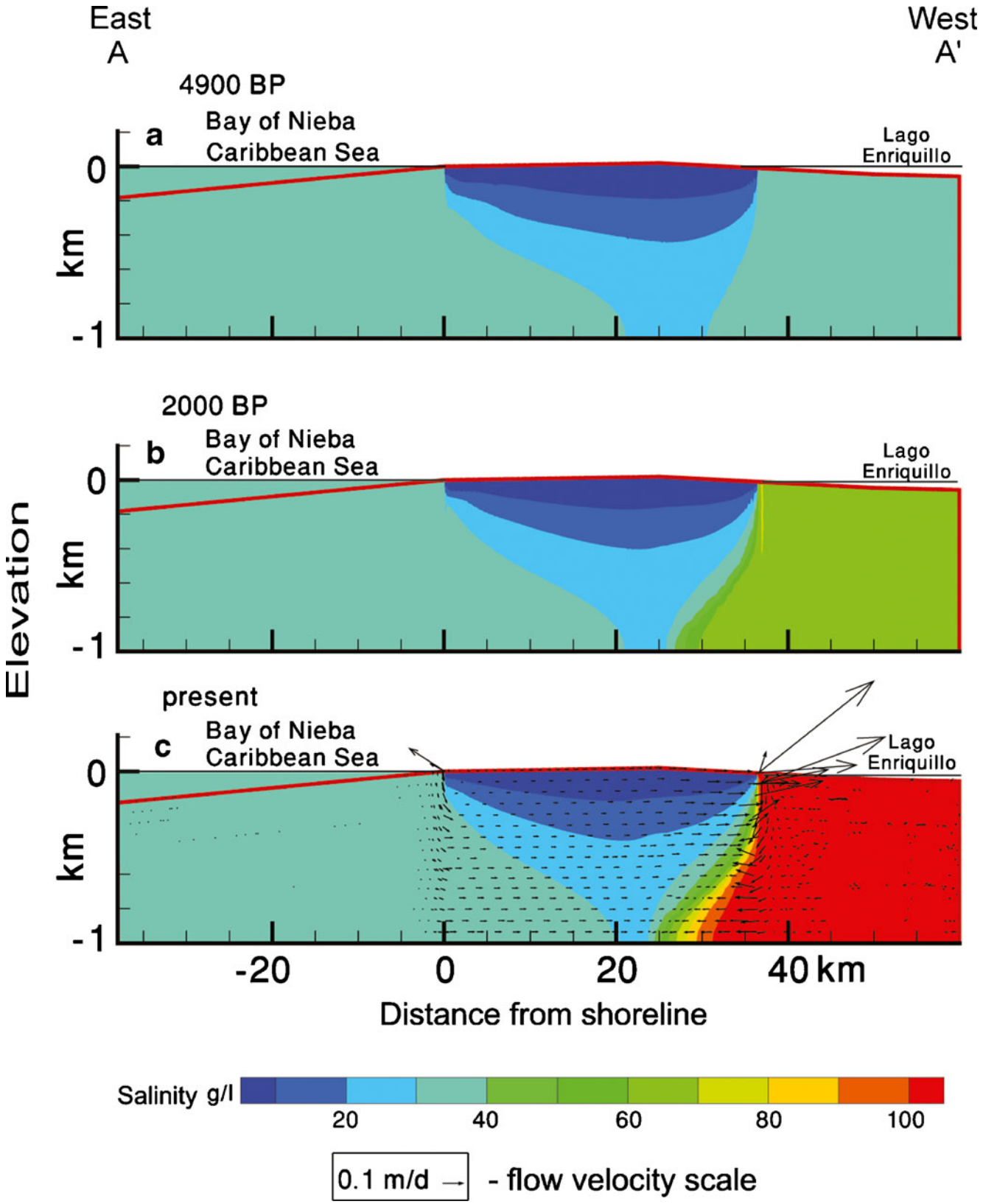

Fig. 8 Transient simulations of the salinity field changes between the sea and Lago Enriquillo in relation to lake level changes

contains more concentrated (present day) brine. The configuration is basically a multiple hydrological system, whereby seawater encroaches into the lake area and the brine is density-driven to some distance in the opposite direction.

 DOI 10.1007/s10040-013-0972-5

Here also, similarly to the case of Lake Asal, the gradual drop of the endorheic base level since 4,900 ka at an average rate of ca. 1 m per hundred years is accompanied in the transient simulations by arrival to a steady state within around 200 years. Namely, the kinetics of the salinity changes of the seawater intrusion and the density-driven brine flow is fast relative to the rate of the base level drop.

Summary and conclusions

The results of numerical simulations presented in this study support the feasibility of seawater encroachment into deep endorheic saline base levels below sea level. Two case studies examined herein, Lake Asal and Lago Enriquillo, were found to enable seawater encroachment into them. The common feature to these cases is an endorheic base level considerably below sea level, which is close to the sea and coupled with a rather low divide in between.

The climatic effect is important in controlling the obtained hydrological configuration. An arid or a semi-arid climate (e.g., Lake Asal) results in low recharge and in turn a low divide, allowing seawater intrusion. Such a climate is also responsible for the high water salinities in the endorheic base level due to high evaporation (e.g., Lake Asal).

The setup described in the preceding leads to a hydrological configuration, as shown schematically in Fig. 1. It consists of an upper freshwater body that drains to both base levels, controlled by the fresh groundwater heads. Underneath it, seawater encroaches all the way from the sea to the lower inland base level whereby the geometry of the fresh/seawater interface formed is controlled by the elevation difference between both base levels, by the freshwater heads and by the densities of the two water bodies involved. Below it, in some cases such as Lake Asal, an interface is recognized between the encroaching seawater body and a brine body underneath, formed through evaporation in the lower base level and which is density-driven backwards toward the sea.

The kinetics of the processes is rather fast. It takes less than a few thousand years to transform a freshwater lake to a hypersaline endorheic base level following its decline below sea level, as a result of seawater encroachment and evaporation. The same short time span is required to enable a considerable density-driven backward flow of the brine.

The effect of high heat flow underneath the Lake Asal system was analyzed numerically in the simulations with coupled heat and mass transport. Interaction between heat advection and flow pattern associated with the fresh/seawater interface leads to a reverse shape of the temperature curve as observed in several boreholes near Lake Asal (e.g., Asal 5 well). The depth-temperature curve is "distorted" at the depth interval of the fresh/seawater interface. This is interpreted herein as a cooling effect of the encroaching fast-flowing and relatively cool seawater, forming a reversal in the temperature curve.

Acknowledgements Thanks are due to Batsheva Cohen from the Geological Survey of Israel who helped with the drafting of the figures. Thanks are also due to associate editor Ward E. Sanford, editor Vincent Post, reviewer Tracy Nishikawa and to anonymous reviewers who contributed to the improvement of the manuscript.

References

Allard P, Tazieff H, Dajlevic D (1979) Observations of seafloor spreading in Afar during the November 1978 fissure eruption. Nature 279:30–33

Ataie-Ashtiani B, Volker RE, Lockington DA (1999) Tidal effects on sea water intrusion in unconfined aquifers. J Hydrol 216:17–31

Audin L, Manighetti I, Tapponnier P, Metivier F, Jacques E, Huchon P (2001) Fault propagation and climatic control of sedimentation on the Ghoubbet Rift Floor: insights from the Tadjouraden cruise in the western Gulf of Aden. Geophys J Int 144:1–28

Ayele A, Nyblade AA, Langston CA, Cara M, Leveque J-J (2006) New evidence for Afro-Arabian plate separation in southern Afar. In: Yirgu G, Ebinger CG, Maguire PKH (Eds) The Afar Volcanic Province within the East African Rift System. Geol Soc Lond Spec Publ 259: 133–141

Bear J, Cheng AH-D, Sorek S, Quazar D, Herrera I (eds) (1999) Seawater intrusion in coastal aquifers: concepts, methods and practices. Kluwer, Dordrecht, The Netherlands

Bobba AG (1993) Mathematical models for saltwater intrusion in coastal aquifers. Water Resour Manag 7:3–37

Bobba AG (2002) Numerical modelling of salt-water intrusion due to human activities and sea-level changes in the Godavari Delta, India. Hydrol Sci J 47:S67–S80

Brewer PG, Spencer DW (1969) A note on the chemical composition of the Red Sea brines. In: Degens ET, Ross DA (eds) Hot brines and recent heavy metal deposits in the Red Sea. Springer, New York, pp 174–179

Buck WR (2006) The role of magma in the development of the Afro-Arabian Rift System. In: Yirgu G, Ebinger CG, Maguire PKH (Eds) The Afar Volcanic Province within the East African Rift System. Geol Soc Lond Spec Publ 259:43–54

Buck DG, Brenner M, Hodell DA, Curtis JH, Martin JB, Pagani M (2005) Physical and chemical properties of hypersaline Lago Enriquillo, Dominican Republic. Verh Int Verein Limnol 29:1–7

Chen BF, Hsu SM (2004) Numerical study of tidal effects on seawater intrusion in confined and unconfined aquifers by time-independent finite-difference method. J Water Port Coastal Ocean Eng 130:191–206

Chiesa S, Mazzoleni G (2001) Dominican Republic (Hispaniola Island, north-eastern Caribbean): a map of morpho-structural units at a scale 1:500,000 through LANDSAT TM image interpretation. Rev Geol Am Cent 25:99–106

Craig H (1969) Geochemistry and origin of the Red Sea brines. In: Degens ET, Ross DA (eds) Hot brines and recent heavy metal deposits in the Red Sea. Springer, New York, pp 208–242

D'Amore F, Giusti D, Abdallah A (1998) Geochemistry of the high-salinity geothermal field of Asal, Republic of Djibouti, Africa. Geothermics 27:197–210

DeMets C, Wiggins-Grandison M (2007) Deformation of Jamaika and motion of the Gonave microplate from GPS and seismic data. Geophys J Int 168:362–378

Diersch H-JG, Kolditz O (2002) Variable-density flow and transport in porous media: approaches and challenges. Adv Water Resour 25:899–944

Doss WC, Greer L, Curran HA, Patterson WP, Mortlock RA (2005) Large tufa-coated serpulid mounds signal and abrupt mid-Holocene transition from marine to restricted hyposaline conditions, Lago Enriquillo, Dominican Republic. Geol Soc Am Abstr with Programs. 37(7):365

 DOI 10.1007/s10040-013-0972-5

Doubre C, Peltzer G (2007) Fluid-controlled faulting process in the Asal Rift, Djibouti, from 8 yr of radar interferometry observations. Geology 35:69–72

Elmi D (2005) Analysis of geothermal well test data from the Asal Rift area, Republic of Djibouti. UN Univ. Geothermal Training Programme Rep. 6, UNU-GTP, Reykjavík, Iceland

Essaid HI (1990) A multilayered sharp interface model of coupled freshwater and saltwater flow in coastal systems: model development and application. Water Resour Res 26:1431–1454

Faure H, Walter RC, Grant DR (2002) The coastal oasis: ice age springs on emerged continental shelves. Glob Planet Chang 33:47–56

Fouillac AM, Fouillac C, Cesbron F, Pillard F, Legendre O (1989) Water–rock interaction between basalt and high-salinity fluids in the Asal Rift, Republic of Djibouti. Chem Geol 76:271–289

Garfunkel Z, Beyth M (2006) Constraints on the structural development of Afar imposed by the kinematics of the major surrounding plates. In: Yirgu G, Ebinger CG, Maguire PKH (eds) The Afar Volcanic Province within the East African Rift System. Geol Soc Lond Spec Publ 259:3–42

Gasse F, Fontes J-C (1989) Palaeoenvironments and palaeohydrology of a tropical closed lake (Lake Asal, Djibouti) since 10,000 year BP. Palaeogeogr Palaeoclimatol Palaeoecol 69:67–102

Gasse F, Rognon P, Street FA (1980) Quaternary history of the Afar and Ethiopian Rift lakes. In: Williams MAJ, Faure H (eds) The Sahara and the Nile: Quaternary environments and prehistoric occupation in northern Africa. Balkema, Rotterdam, The Netherlands, pp 361–400

Ghyben WB (1888) Notes on the probable resultsof well drilling near Amsterdam (in Dutch). Tijdschrift van het Koninklijk Inst. van Ingenieur, The Hague 9:8–22

Harrar WG, Williams AT, Barker JA, Camp MV (2001) Modeling scenarios for the emplacement of palaeowaters on aquifer systems. In: Edmunds WM, Milne CJ (eds) Palaeowaters in coastal Europe: evolution of groundwater since the late Pleistocene. Geol Soc London Spec Publ 189: 213–229

Herzberg B (1901) Die wasserversorgung einiger Nordseebader [The water supply of some North Sea resorts]. J Gasbeleucht Wasservesorg 44(815–819):824–844

Houssein DE, Axelsson G (2010) Geothermal resources in the Asal Region, Republic of Djibouti: an update with emphasis on reservoir engineering studies. Geothermics 39:220–227

Jalludin M, Razack M (1994) Analysis of pumping tests, with regard to tectonics, hydrothermal effects and weathering, for fractured Dalha and stratiform basalts, Republic of Djibouti. J Hydrol 155:237–250

Kafri U (1984) Current subsurface seawater intrusion to base levels below sea level. Environ Geol Water Sci 6:223–227

Kafri U, Arad A (1979) Current subsurface intrusion of Mediterranean seawater: a possible source of groundwater salinity in the Rift Valley System. Israel J Hydrol 44:267–287

Kafri U, Yechieli Y (2010) Groundwater base level changes and adjoining hydrological systems. Springer, Heidelberg

Kafri U, Goldman M, Lyakhovsky V, Scholl C, Helwig S, Tezkan B (2007) The configuration of the fresh–saline groundwater interface within the regional Judea Group carbonate aquifer in northern Israel between the Mediterranean and the Dead Sea base levels as delineated by deep geoelectromagnetic soundings. J Hydrol 344:123–134

Kooi H, Groen J, Leijnse A (2000) Modes of seawater intrusion during transgressions. Water Resour Res 36:3581–3589

Manighetti I, Tapponnier P, Courtillot V, Gallet Y (2001) Strain transfer between disconnected, propagating rifts in Afar. J Geophys Res 106:13613–13665

Mann P, Taylor FW, Burke K, Kulstad R (1984) Subaerially exposed Holocene coral reef, Enriquillo Valley, Dominican Republic. Geol Soc Am Bull 95:1084–1092

Medley PR (2006) Paleohydrology of middle Holocene lagoonal & lacustrine deposits in the Enriquillo Valley, Dominican Republic: pore morphometrics and isotope geochemistry of Ostracoda. Geol Soc Am Abstr with Programs 38:444

Mlynarski M, Zlotnicki J (2001) Fluid circulation in the active emerged Asal rift (east Africa, Djibouti) inferred from self-potential and Telluric-Telluric prospecting. Tectonophysics 339:455–472

Morillo HR, Huertas JFF (2006) Potencial hidrogeologico de la Republica Dominicana [The hydrogeological potential of the Dominican Republic]. Bol Geol Min 117:187–200

Olin M (1995) Estimation of base level from an aquifer from recession rates of groundwater levels. Hydrogeol J 3:40–51

Pizzi A, Coltorti M, Abebe B, Disperati L, Sacchi G, Salvini R, (2006) The Wonji fault belt (Main Ethiopian Rift): structural and geomorphological constraints and GPS monitoring. In: Yirgu G, Ebinger CG, Maguire PKH (Eds) The Afar Volcanic Province within the East African Rift System. Geol Soc Lond Spec Publ 259:191–207

Reilly TR, Goodman AS (1985) Quantitative analysis of saltwater-freshwater relationship in groundwater systems: a historical prespective. J Hydrol 80:125–160

Sanjuan B, Michard G, Michard A (1990) Origine des substances dissoutes dans les eaux des sources thermals et des forages de la region Asal-Ghoubbet (Republique de Djibouti) [The origin of solute substances of the thermal water sources in the wells of the Asal-Ghoubbet region (Republic of Djibouti)]. J Volcanol Geotherm Res 43:333–352

Schoell M, Faber E (1978) New isotopic evidence for the origin of Red Sea brines. Nature 275:436–438

Tarantola A, Ruegg JC, Lepine JP (1980) Geodetic evidence for rifting in Afar, 2: vertical displacements. Earth Planet Sci Lett 48:363–370

Tuttle MP, Prentice CS, Dyer-Williams K, Pena LR, Burr G (2003) Late Holocene liquefaction features in the Dominican Republic: a powerful tool for earthquake hazard assessment in the northeastern Caribbean. Seismol Soc Am Bull 93:27–46

Winsor K, Curran HA, Greer L, Glumac B (2006) Paleoenvironmental implications of mid-Holocene serpulid tube/tufa mounds and underlying coral colonies, Enriquillo Valley, Dominican Republic. Geol Soc Am Abstr with Programs 38:68

Wright TJ, Ebinger C, Biggs J, Ayele A, Yirgu G, Keir D, Stork A (2006) Magma-maintained rift segmentation at continental rupture in the 2005 Afar dyking episode. Nature 442:291–294

 DOI 10.1007/s10040-013-0972-5